arXiv:cond-mat/0201330v1 [cond-mat.mes-hall] 18 Jan 2002

Model Exact Low-Lying States and Spin Dynamics in Ferric Wheels; Fe_6 to Fe_{12}

Indranil Rudra[1], **S. Ramasesha**[1] **and Diptiman Sen** [2]

[1]Solid State and Structural Chemistry Unit

Indian Institute of Science, Bangalore 560 012, India

[2] Centre for Theoretical Studies

Indian Institute of Science, Bangalore 560 012, India

Using an efficient numerical scheme that exploits spatial symmetries and spin-parity, we have obtained the exact low-lying eigenstates of exchange Hamiltonians for ferric wheels up to Fe_{12}. The largest calculation involves the Fe_{12} ring which spans a Hilbert space dimension of about 145 million for M_s=0 subspace. Our calculated gaps from the singlet ground state to the excited triplet state agrees well with the experimentally measured values. Study of the static structure factor shows that the ground state is spontaneously dimerized for ferric wheels. Spin states of ferric wheels can be viewed as quantized states of a rigid rotor with the gap between the ground and the first excited state defining the inverse of moment of inertia. We have studied the quantum dynamics of Fe_{10} as a representative of ferric wheels. We use the low-lying states of Fe_{10} to solve exactly the time-dependent Schrödinger equation and find the magnetization of the molecule in the presence of an alternating magnetic field at zero temperature. We observe a nontrivial oscillation of magnetization which is dependent on the amplitude of the *ac* field. We have also studied the torque response of Fe_{12} as a function of magnetic field, which clearly shows spin-state crossover.

PACS numbers: 75.45.+j, 75.50.Xx, 75.60.Ej

I. INTRODUCTION

In recent years polyoxometalates which are practical realization of nanomagnets have become the area of intense research because of their enormous variety of structure and fascinating magnetic properties. A particular aesthetic class is that of the ring-shaped iron(III) compounds denoted as molecular ferric wheels. The decanuclear wheel Fe_{10} synthesized by Lippard et. al.[1] may be regarded as a prototype of this class. Meanwhile synthesis of ferric wheels with 6, 8, 12 and 18 have also been reported[2]. These materials have dominant anti-ferromagnetic coupling between Fe(III) spins and a singlet ground state. The magnetic properties of such nanoscopic molecules result from the interplay of superexchange interactions between the atomic spins, dipolar coupling of the local moments and on-site anisotropies arising from ligand configurations. The emergence of ferric wheels has led to a renewed interest in the properties of the Heisenberg chain, especially for large spin values. In 1964 Fisher used a classical treatment[3], in which spin quantization

is absent, to study the properties of Heisenberg Hamiltonian and found analytical solutions for the thermodynamic properties of the system. Numerous quantum mechanical calculations have been made for Heisenberg Hamiltonian, mostly for spin-1/2 chains. Calculations for larger S became more interesting after Haldane's conjecture[4] regarding the presence of an energy gap in the excitation spectrum from the ground state for integer S chains.

To fit the experimental temperature dependence of the magnetic susceptibility data for Fe_{10} Lippard et. al. adopted a classical spin treatment to obtain the value of exchange interaction parameter J. But below 50 K this treatment fails. Ferric wheels with S=5/2, and system size of up to 8 sites have been treated exactly using irreducible tensor operator technique[5] with the aid of point group symmetry as well as by using the invariance of spin Hamiltonian with regard to interchange of spin sites[6]. Recently there have been theoretical studies to explain the low temperature magnetic susceptibility data of Fe_{10}[7]. The magnetization of ferric wheels exhibit a step like field dependence at low temperature due to the occurrence of field induced ground state level crossing, a spectacular manifestation of quantum size effect in these nanomagnets[1,8]. There have been NMR and specific heat studies of these ferric wheels to investigate the energy level structure[9,10]. In appropriate parameter regime these ring systems are considered to be the candidates for the observation of macroscopic quantum phenomena, in the form of quantum coherent tunneling of the Neel vector[11]. To understand these low temperature properties of ferric wheels in detail we need to know the low lying eigenvalue spectrum for these systems. It is also of interest to compare and contrast the zero temperature density of state of S=5/2 rings with that of the exactly known S=1/2 chain. In this paper we have used spin parity together with rotational symmetry of the ferric wheels to obtain the low-lying eigenvalue spectrum for rings with 6, 8, 10 and 12 spin-5/2. The dispersion spectrum reveals interesting features. There have been recent reports of solving the low-lying eigen-spectrum of Fe_{10} using the Density Matrix Renormalization Group[12]. To the best of our knowledge ours is the first study of of ferric wheels using exact methods up to a ring size of 12, S=5/2 iron(III) ions.

We have also studied the quantum spin dynamics of ferric wheels in presence of an alternating field after setting up the Hamiltonian matrix in the subspace of low-lying states. This Hamiltonian includes multipolar spin-spin interaction terms besides a time varying magnetic field (Zeeman term). We have then evolved an initial state, which is taken to be the ground state with a specific value of M_S (the z-component of the total spin) in the absence of the magnetic field, by using the time-dependent formulation of the problem in the restricted subspace. We observe a nontrivial oscillation of the magnetization whose frequency depends on the amplitude of the alternating field. This phenomena is very similar to what has been observed in case of uniaxial magnets[13].

II. MODEL HAMILTONIAN AND COMPUTATIONAL DETAILS

A. Symmetry Adaptation of Correlated States

The full symmetry of electronic states is of central interest in quantum theory. Since nonrelativistic Hamiltonians $\hat{H}$ does not depend explicitly on spin, molecular eigenstates can be labeled by the total spin S and the appropriate irreducible representation of the point group. The model Hamiltonian employed in this study is the isotropic exchange Hamiltonian involving exchange interaction between nearest neighbors,

$$\hat{H} = \sum_{<ij>} J_{ij} \hat{s}_i \cdot \hat{s}_j \tag{1}$$

where the exchange interaction J_{ij} takes the values dictated by experimental studies of structure and magnetic properties. For Fe_6 the J value depends on the central alkali metal atom : for Na:Fe_6 J=32.77 K whereas for Li:Fe_6 J=20.83 K. In Fe_8, Fe_{10} and Fe_{12} J is 22 K,15.56 K and 31.97 K respectively[14].

The total dimensionality of the Fock space of the ferric wheel is given by

$$D_F = \prod_{1}^{n} (2S_i + 1) \tag{2}$$

where 'n' is the total number of spins in the wheel and S_i is the spin on each ion. In case of Fe_{10}, there are 10 iron(III) ions with the dimensionality of the Fock space 60,466,176. In case of Fe_{12}, which we have solved exactly this dimension is 2,176,782,336.

Specializing to given total M_S leads to Hilbert space dimensionalities which are lower than the Fock space dimensionality. In the case of the Fe_{12} cluster the $M_S = 0$ space has a dimensionality of about 145 million (144,840,476). The major challenge in exact computation of the eigenvalues, and properties of these spin clusters lies in handling such large bases and the associated matrices. While the dimensions look overwhelming, the matrices that represent the operators in these spaces are rather sparse. Usually, the number of nonzero elements in a row is of the order of the number of exchange constants in the Hamiltonian. This sparseness of the matrices allows one to handle fairly large systems. However, in the case of spin problems, generating the bases states and using the symmetries of the problem is nontrivial.

The isotropic exchange Hamiltonians conserve total spin, S, besides the z-component of the total spin, M_S. Besides these symmetries, the geometry of the cluster also leads to spatial symmetries which can often be exploited. The simplest way of generating bases functions which conserve total spin is the VB method that employs the Rumer-Pauling rule[15]. It is quite easy to generalize the Rumer-Pauling rules to a cluster consisting of objects with different spins to obtain states with

desired total spin, S. However, setting-up the Hamiltonian matrix in such a basis can be computationally intensive since the exchange operators operating on a "legal" VB diagram (diagram that obeys Rumer-Pauling rules) could lead to "illegal" VB diagrams and resolving these "illegal" VB diagrams into "legal" diagrams would present the major bottle-neck. Indeed, the same difficulty is encountered when spatial symmetry operators operate on a VB function. Thus, the extended VB methods are not favored whenever one wishes to apply it to a motley collection of spins or when one wishes to exploit some general spatial symmetries that may exist in the cluster[16].

It is advantageous to partition the spaces into different total spin spaces because of the usually small energy gaps between total spin states which differ in S by unity. To avoid the difficulties involved in working with total spin eigenfunctions, we exploit parity symmetry in the systems. The parity operation involves changing the z-component of all the spins in the cluster from $\mathrm{M_{S_i}}$ to $-\mathrm{M_{S_i}}$. There is an associated phase factor with this operation given by $(-1)^{\mathrm{S_{tot}}+\sum_{\mathrm{i}}\mathrm{S_i}}$. The isotropic exchange operator remains invariant under this operation. If this symmetry is employed in the $\mathrm{M_S} = 0$ subspace, the subspace is divided into "even" and "odd" parity spaces depending upon the sign of the character under the irreducible representation of the parity group. The space which corresponds to even (odd) total spin we call the even (odd) parity space. Thus, employing parity allows partial spin symmetry adaptation which separates successive total spin spaces, without introducing the complications encountered in the VB bases. However, the VB method can lead to complete factorization of the spin space leading to smaller complete subspaces.

In the ferric wheels, besides spin symmetries, there also exists spatial symmetries. The topology of the exchange interaction leads to a $\mathrm{C_n}$ point group symmetry, where 'n' is the number of iron ions in the ring. Hence, $\mathrm{Fe_6}, \mathrm{Fe_8}, \mathrm{Fe_{10}}, \mathrm{Fe_{12}}$ will have $\mathrm{C_6}$, $\mathrm{C_8}$, $\mathrm{C_{10}}$ and $\mathrm{C_{12}}$ symmetry respectively. It should be mentioned that among these ferric wheels only $\mathrm{Fe_{10}}$ is strictly having a ten fold rotational symmetry, rest of them approximately have the above mentioned symmetry. For computational advantage we have assumed the rotational symmetry for all the ferric wheels. This point group appears at first site to present difficulties because the characters in the irreducible representation are in some cases complex which could lead to complex bases functions. This, however, can be avoided by recognizing that in the $\mathrm{C_n}$ group, states with wavevectors 'k' and '-k' are degenerate. We can therefore construct a linear combination of the 'k' and '-k' states which is real. The symmetry representations in the $\mathrm{C_n}$ group would then correspond to the labels A, B and E, with the characters in the E representation given by $2\cos(rk)$ under the symmetry operation $\mathrm{C_n^r}$, with $\mathrm{k} = \pi/\mathrm{n}$. The parity operation commutes with the spatial symmetry operations and the full point group of the system would then correspond to the direct product of the two groups. Since both parity and spatial symmetries can be easily incorporated in a constant $\mathrm{M_S}$ basis, we do not encounter the difficulties endemic to the VB theory.

The generation of the complete basis in a given Hilbert space requires a simple representation of a state on the computer. This is achieved by associating with every state a unique integer. In this integer, we associate n_i bits with spin s_i, such that n_i is the smallest integer for which $2^{n_i} \geq (2s_i + 1)$. In the integer that represents the state of the cluster, we ensure that these n_i bits do not take values which lead to the n_i bit integer value exceeding $(2s_i + 1)$. For each of the allowed bit states of the n_i bit integer, we associate an M_{S_i} value between $-s_i$ and s_i. For a spin cluster of 'n' spins, we scan all integers of bit length $N = \sum_{i=1}^{n} n_i$ and verify if it represents a basis state with the desired M_S value. In Fig. 1, we show a few basis functions with specified M_s value for some typical ferric wheels along with their bit representations and the corresponding integers. Generation of the bases states is usually a very fast step, computationally. Generating the basis as an ordered sequence of integers that represent them also allows for rapid generation of the Hamiltonian matrix elements as will be seen later.

Symmetrization of the basis by incorporating parity and spatial symmetries involves operation on the constant $M_S = 0$ basis by the symmetry operators. Since spatial symmetry operators permute the positions of equivalent spins, every spatial symmetry operator operating on a basis function generates another basis function. Every symmetry operator can be represented by a correspondence vector whose i^{th} entry gives the state that results from operating on the i^{th} state by the chosen operator. This is also true for the parity operator, in the $M_S = 0$ subspace.

The first step in constructing symmetry adapted linear combinations is to represent the symmetry operators in the chosen basis as matrices. In our case, the symmetry operators are such that symmetry operation by any operator on a basis state leads to a resultant which is a single basis state. Thus all our symmetry operators can be represented as vectors; the entry in position 'i' gives the index of the basis function generated by symmetry operation on the basis state 'i'. Since the basis is very large, it is prohibitive to store and manipulate the full basis together with all the associated symmetry vectors. To avoid these difficulties, we have constructed the symmetry matrices in small invariant subspaces. These invariant subspaces are obtained by sequentially choosing a state and operating on it by all the symmetry operators. This gives rise to a set of states on which we again operate by all the symmetry operators, and continue this process until no new basis states are generated. The collection of all these basis states resulting at the end of this process is the invariant subspace. We can set-up symmetry combinations of the basis states in each of the invariant subspaces independently. The symmetry combinations can now be obtained operating on each state by the group theoretic projection operator,

$$\hat{P}_{\Gamma_i} = \frac{1}{h} \sum_R \chi_{\Gamma_i}(R)\hat{R} \tag{3}$$

on each of the basis states of the invariant subspace. Here Γ_i is the i^{th} irreducible representation,

$\hat{R}$ is the symmetry operation of the group and $\chi_{\Gamma_i}(R)$ is the character under $\hat{R}$ in the irreducible representation Γ_i. This process is repeated with the next basis state that has not appeared in any of the invariant subspaces already constructed. The process comes to an end when all the basis states have appeared in any one of the invariant subspaces.

The resulting symmetrized basis is usually over complete in each of the invariant subspaces. The linear dependencies can be eliminated by a Gram-Schmidt orthonormalization procedure. However, in most cases, ensuring that a given basis function does not appear more than once in a symmetrized basis is sufficient to guarantee linear independence and weed out the linearly dependent states. A good check on the procedure is to ensure that the dimensionality of the symmetrized space in the invariant subspace agrees with that calculated from the traces of the reducible representation obtained from the matrices corresponding to the symmetry operators in the chosen invariant subspace. Besides, the sum of the dimensionalities of the symmetrized spaces should correspond to the dimensionality of the unsymmetrized invariant subspace in each of these subspaces.

Generation of the Hamiltonian matrix is rather straight forward and involves operation of the Hamiltonian operator on the symmetry adapted basis. This results in the matrix **SH**, where **S** is the symmetrization matrix representing the operator $\hat{P}_{\Gamma_i}$ and **H** is the matrix whose elements h_{ij} are defined by

$$\hat{\mathrm{H}}|\mathrm{i}>=\sum_{\mathrm{j}} \mathrm{h_{ij}}|\mathrm{j}> . \tag{4}$$

The states {i} correspond to the unsymmetrized basis functions. The Hamiltonian matrix in the symmetrized basis is obtained by right multiplying the matrix **SH** by $\mathbf{S}^{\dagger}$. The resulting symmetric Hamiltonian matrix is stored in the sparse matrix form and the matrix eigenvalue problem is solved using the Davidson algorithm[17].

Computation of the properties is easily done by transforming the eigenstate in the symmetrized basis into that in the unsymmetrized basis. Since the operation by any combination of spin operators on the unsymmetrized basis can be carried out, all relevant static properties in different eigenstates can be obtained in a straightforward manner.

B. Quantum Spin Dynamics

We have studied the dynamics in ferric wheels by setting up the Hamiltonian matrix in the desired $\mathrm{M_S}$ space, which in all cases is restricted to $\mathrm{M_S} = 0, 1$ and 2. In each subspace we have obtained a few low-lying states using the Davidson algorithm[17]. We have also calculated the spin-spin correlation functions in each of the states. Using the spin-spin correlation functions, we have

computed the expectation value of $S^2_{\rm total}$ operator, from which we have identified the total spin of the state. We observe from the eigenvalue spectrum of all the ferric wheels that ground state and the first excited state are spin singlet (S=0) and triplet (S=1) state respectively, they belong to two different spatial symmetry subspaces. So they will not mix unless there is a perturbation which spoils the C_{10} symmetry of the molecule. We also notice that the first (triplet) and the second (quintet) excited states again fall into different symmetry subspaces. This is true in all the ferric wheels we have studied.

To study quantum dynamics we have considered the following Hamiltonian[18],

$$\hat{\rm H} = {\rm E_s} - {\rm D}\ \hat{\rm S}^2_{\rm z,total} + {\rm c}\ (\hat{\rm S}^2_{\rm x,total} - \hat{\rm S}^2_{\rm y,total}) - {\rm g}\ {\rm h(t)}\ \hat{\rm S}_{\rm z,total} \tag{5}$$

Here D is the quadratic anisotropy factor, g is the Landé g-factors for the iron(III) spin respectively, and h(t) is the time-dependent magnetic field, expressed as ${\rm h(t)} = {\rm H_0}\cos(\omega {\rm t})$, where ω is the frequency at which field is ramped and $\rm H_0$ is the amplitude of the field. We have chosen ${\rm D} = 8.8 \times 10^{-3}$ and ${\rm c} = 10^{-3}$ (in units of J) in accordance with the experimental values for Fe_{10}. We take $g = 2.0$. The constants $\rm E_s$ in Eq. (5) correspond to the lowest energies obtained from Eq. (1). The second order anisotropy term allows transitions between states with $\Delta {\rm M_S} = \pm 2$. Both second and third terms in Eq. (5) arises due to magnetocrystalline anisotropy. The exact form of the anisotropy in ferric wheel is not very well established. We have included anisotropy terms only up to second order in the spin variables. The anisotropy in the plane can be formed artificially, e.g. by means of external electric or magnetic fields, pressure or using anisotropic substrate[18].

The Hamiltonian in Eq. (5) does not allow the mixing of the (singlet) ground state, (triplet) first excited state and (quintet) second excited state in Fe_{10} because of symmetry reason already mentioned earlier. To observe spin dynamics we apply a constant magnetic field that leads to triplet being the ground state of the system. This constant shifting field plays here the role of a chemical potential and is used to provide the optimal conditions for observing the considered quantum spin dynamics. We can represent the external field as

$$\rm B \ = \ B_0 \ + \ H_0 \cos(\omega t) \tag{6}$$

To study the evolution of magnetization as a function of applied oscillatory field we start from a fixed axial field amplitude (in units of $\rm J/\hbar$) and time is increased in small time step of $\Delta {\rm t} = 0.01$ ($\hbar$/J), frequency of the field is kept constant.

We have studied the time evolution of the system by solving the time-dependent Schrödinger equation,

$$i\hbar \frac{{\rm d}\psi}{{\rm dt}} = \hat{\rm H}({\rm t})\psi \ . \tag{7}$$

We assume the system to be in the state with $S = 1,\ M_S = -1$ at time $t = 0$. This is the initial state which is time evolved according to the equation

$$\psi(t + \Delta t) = e^{-i\hat{H}(t+\frac{\Delta t}{2})\Delta t/\hbar}\ \psi(t)\ . \tag{8}$$

The evolution is carried out by explicit diagonalization of the Hamiltonian matrix $\mathbf{H}(t + \frac{\Delta t}{2})$, and using the resulting eigenvalues and eigenvectors to evaluate the matrix of the time evolution operator $e^{-i\hat{H}(t+\frac{\Delta t}{2})\Delta t/\hbar}$. We set up the Hamiltonian matrix for time evolution in the truncated basis of 3 states corresponding to total spin S=1. We repeatedly carry out the the time evolution in small time steps of size Δt to obtain time evolution over longer periods.

III. RESULTS AND DISCUSSION

A. Analysis of Low-lying Spectrum

We have solved the exchange Hamiltonian (Eq. (1)) exactly using the method mentioned earlier to obtain the low-lying eigenvalue spectrum for 6, 8, 10 and 12 site iron(III) rings. We find that ground state, first, second and third excited states are respectively singlet, triplet, quintet and heptet for all ferric wheels. We notice that there is no accidental degeneracy between the energy levels belonging to different symmetry subspaces. Ground state switches between A^+ (k =0) and B^+ (k = π) subspace for even and odd value of 'm' respectively, in N=2m ring systems. This was also observed by Mattheiss in case of a spin-1/2 chain and can be understood from Marshall's sign rule. The gap between the ground state and the first excited state is shown in Fig. 2 as a function of inverse ring size. According to Haldane conjecture, the gap should extrapolate to zero. The extrapolated value, while small is still finite, suggesting that in these rings the finite size effects are still at play at the ring sizes we have studied.

Using the exchange constants estimated for the different ring systems, we estimate the gap between the ground state and the first excited state to be 22.67 K, 11.81 K, and 6.88 K for Na : Fe_6, Fe_8, Fe_{10} respectively. Our calculated values compare very well with the experimental values, which are 22.0 K, 12.1 K and 6.45 K for Na : Fe_6, Fe_8 and Fe_{10} respectively[14]. This agreement shows that for all practical purposes ferric wheels can safely be assumed as rings neglecting the slight deviation from the exact circular geometry. Our calculated gap for and Fe_{12} is 12.09 K corresponding to the exchange constants predicted from experiments. However, experimental estimate of this gap is lacking.

If we define δ_i to be the energy difference between the i-th excited state and the ground state,

we find from Fig. 3 that the following relationship is satisfied for the ferric wheels,

$$\delta_i \;=\; \frac{S_i(S_i \;+\; 1)}{2} \times E_1 \tag{9}$$

where E_1 is the energy gap between the ground state and the first excited state. This indicates that the lowest spin state obeys the Lande interval rule, in agreement with Taft's conjecture. If we assume E_1 to be the inverse of the moment of inertia, then the above expression gives the rotational energy of a rigid rotor in a state with quantum number S_i. Thus, the spin states of ferric wheels can be viewed as the quantized states of a rigid rotor.

In Fig. 4 we have shown the dispersion spectrum of ferric wheels. The value of k corresponding to a wavefunction ψ can be defined as,

$$T\psi \;=\; e^{ik}\psi \tag{10}$$

where T is the translation operator which in case of a ring rotates the ring by one lattice spacing. We have used the spatial C_n symmetry of the ferric wheels, which enables us to identify the value of k easily for a specified eigenfunction. We find that, in the momentum (k) sector which contains the ground state, the lowest excitation is to a quintet state. For all the other k-sectors the lowest excitation is to a triplet state. Previous studies[19] on antiferromagnetic spin-1/2 Heisenberg chains show that the excitation spectrum is given by $\hbar\omega \;=\; (\pi/2)J|\sin k|$, where k is the wave vector of the excited states measured with respect to that of the ground state. The simple antiferromagnetic spin-wave theory based on the use of the Holstein-Primakoff transformation for each sublattice, leads to excitation spectrum (S is the magnitude of the individual spin S_i),

$$\hbar\omega \;=\; 2\; J\; S\; |\sin k|. \tag{11}$$

This relation is supposed to be correct for $S \rightarrow \infty$. We notice that the excitation spectrum for ferric wheels can be fitted to a $|\sin k|$ kind of function. Data points in k=0 or $k = \pi$ diverges from the above sinusoidal function. This may be a finite size effect. In the thermodynamic limit of infinite chain length excitation spectrum of ferric wheel will be similar to Eq. (11).

We have also calculated the spin-spin correlation function ($\sum_{ij} < S_i^z S_j^z >$) of ferric wheels and Fourier transformed it to find out the structure factor ($S(q)$). In Fig 5.(a - d) we have plotted the structure factor as a function of wave vector q for different symmetry subspaces. In all the cases $S(q)$ shows a peak at $q \;=\; \pi$. The ground state is a Neél ordered state. It also signifies that ground state will undergo a spontaneous distortion with wave vector π. We find that the weight of $S(q)$ is more in case of ground state than excited states.

B. Evolution of Magnetization in presence of an *ac* field

We have studied the evolution of magnetization in presence of an axial *ac* magnetic field varying the amplitude of the field. We have kept the frequency of the field fixed at ω=10^{-3}. We calculate the magnetization at each time step. When we draw a smooth curve for the time evolution over long time periods, we find a sinusoidal motion,

$$M(t) \sim \cos(\Omega t) \tag{12}$$

which can be seen in Fig. 6. Unexpectedly the frequency Ω of this sinusoidal motion does not correspond to an eigenfrequency of the system or to the period of the external field. When we change the amplitude H_0 of the field, the period of the magnetization changes, which is shown in Fig 6. We find a regular dependence of Ω as a function of H_0, as in Fig 7. Frequency of oscillation Ω becomes very small for some values of H_0, again it increases but to a lower value than the previous Ω_{max}. Ω_{max} values can be fitted to a exponentially decaying curve. This nontrivial resonance can be understood from the viewpoint of Floquet's theorem[20]. Nonadiabatic transitions are possible whenever system becomes metastable. This resonance can be observed if two states with different magnetizations are nearly degenerate leading to large tunneling cross sections between the states resulting in oscillation of the magnetization. This magnetization oscillation can be related to that of macroscopic quantum coherence, which is predicted by Zvezdin *et. al.*[18].

C. Torque Magnetometry

Cornia et. al. have used a novel cantilever torque magnetometry technique to study the spin-state crossover in ferric wheels. The torque $\mathbf{T}$ experienced by a magnetically anisotropic substance in a uniform magnetic field $\mathbf{B}$ is given by

$$\mathbf{T} = \mathbf{M} \times \mathbf{B} \tag{13}$$

where $\mathbf{M}$ is the magnetization of the sample. $\mathbf{T}$ vanishes when the magnetic field is applied along one of the principle directions $\hat{x}$, $\hat{y}$, $\hat{z}$ of the susceptibility tensor, since in this case $\mathbf{M}$ and $\mathbf{B}$ are collinear. The $\hat{y}$ component of the torque operator $\mathbf{T}_y$ can be easily obtained for an applied magnetic field of the form

$$\mathbf{B} = B(\cos\theta\hat{z} + \sin\theta\hat{x}), \tag{14}$$

in Eq. 5, and is given by,

$$< \mathbf{T}_y >= -g\mu_B B(< S_x > \cos\theta - < S_z > \sin\theta) \tag{15}$$

where $< S_\alpha > = \sum_{i=1}^{N} < S_{i,\alpha} >$ is the ground state expectation value of the component α of the total spin operator. We have computed $< \mathbf{T}_y >$ for Fe_{12} on the basis of the eigenvectors of the Hamiltonian in Eq. 5. When θ is $\frac{\pi}{4}$ then torque is maximal and $< \mathbf{T}_y >$ is just the difference between the $\hat{x}$ and $\hat{z}$ spin components. In Fig. 8 we have shown the variation of $< \mathbf{T}_y >$ with magnetic field. We can clearly observe the step behavior of the torque component which is a manifestation of the level crossing of singlet,triplet and quintet states.

IV. SUMMARY AND OUTLOOK

We have implemented a general and efficient procedure that allows us to block factorize the spin Hamiltonian matrix based on its invariance under cyclic symmetry and parity operation. This method can be used in general for systems of other symmetries also. We have obtained the low-lying eigenvalue spectrum of ferric wheels up to Fe_{12} using the C_n rotational symmetry of the molecules. We have also analyzed the dispersion spectrum and structure factor. To reproduce the low temperature properties of ferric wheels we need to know the low-lying eigenvalue spectrum of these systems. We have also studied the dynamics of ferric wheel evolving a proper initial state. We observe nontrivial oscillation of magnetization in presence of an alternating magnetic field. We have also obtained the torque of the ferric wheels in the presence of a nonaxial magnetic field and find that the torque also exhibits step like behavior with field. Evidently a study including the effect of nonzero temperature on this oscillation is a challenging problem of future research.

Acknowledgement: We thank CSIR, India and DAE-BRNS, India for financial support.

---

[1] K. L. Taft, C. D. Delfs, G. C. Papaefthymiou, S. Foner, D. Gatteschi and S. J. Lippard, J. Am. Chem. Soc. **116**, 823 (1994).

[2] G. L. Abbati, A. Cornia, A. C. Fabretti and W. Malavasi, Inorg. Chem. **36**, 6443 (1997) ; A. Caneschi, A. Cornia and S. J. Lippard, Angew. Chem. Int. Ed. Engl. **4**, 467 (1995) ; K. L. Taft and S. J. Lippard , J. Am. Chem. Soc. **112**, 9629 (1990) ; R. W. Saalfrank, I. Bernt, E. Uller and F. Hampel, Angew. Chem. **109**, 2596 (1997) ; A. Caneschi, A. Cornia, A. C. Fabretti and D. Gatteschi, Angew. Chem. Int. Ed. Engl. **38**, 1295 (1999).

[3] J. C. Fisher and M. E. Fisher, Phys. Rev. **135**, A640 (1964).

[4] F. D. M. Haldane, Phys. Lett. **93A**, 464 (1983) ; Phys. Rev. Lett. **50**, 1153 (1983) ; I. Affleck, J. Phys. Condens. Matter. **1**, 3047 (1989).

[5] D. Gatteschi and L. Pardi, Gazz. Chim. Ital. **123**, 231 (1993).

[6] O. Waldmann, R. Koch, S. Schromm, J. Schülein, P. Müller , I. Bernt, R. W. Saalfrank, F. Hampel and E. Balthes, Inorg. Chem. **40**, 2986 (2001) ; O. Waldmann, Phys. Rev. B **61**, 6138 (2000).

[7] Juan Bruno and R. J. Silbey, J. Phys. Chem. A **104**, 596 (2000).

[8] A. Cornia, A. G. M. Jansen and M. Affronte, Phys. Rev. B **60**, 12177 (1999).
[9] M. H. Julien, Z. H. Jang, A. Lascialfari, F. Borsa, M. Horvatic, A. Caneschi and D. Gatteschi, Phys. Rev. Lett. **83**, 227 (1999).
[10] M. Affronte, J. C. Lasjaunias, A. Cornia and A. Caneschi, Phys. Rev. B **60**, 1161 (1999).
[11] A. Chilero, D. Loss, Phys. Rev. Lett. **80**, 169 (1998).
[12] B. Normand, X. Wang, X. Zotos and D. Loss, Phys. Rev. B **63**, 184409 (2001).
[13] S. Miyashita, K. Saito and H. De Raedt, Phys. Rev. Lett. **80**, 1525 (1998).
[14] A. Caneschi , D. Gatteschi , C. Sangregorio , R. Sessoli, L. Sorace , A. Cornia , M. A. Novak , C. Paulsen and W. Wernsdorfer, J. Magn. Magn. Mater. **200**, 182 (1999).
[15] For a review see S. Ramasesha and Z.G. Soos, "Valence Bond Theory of Quantum Cell Models", in *Valence Bond Theory and Chemical Structure* Eds. D.J. Klein and D.L. Cooper, Elsevier (Amsterdam) in Press.
[16] S. Ramasesha and Z. G. Soos, J. Chem. Phys. **98**, 4015 (1993)
[17] E.R. Davidson, J. Comput. Phys. **17**, 87 (1975).
[18] A. K. Zvezdin, cond-mat/0004074 .
[19] J. D. Cloizeaux and J. J. Pearson, Phys. Rev. **128**, 2131 (1962).
[20] J. H. Shirley, Phys. Rev. **138**, B979 (1965).

Figure Captions

1. Representative $M_s = 0$ state in (a) 6 spin-$\frac{1}{2}$ cluster (b) Fe_{12} wheel with all the sites having spin $S = \frac{5}{2}$. Numbers in paranthesis correspond to the M_s value at the site. Bit representation as well as the integer value are given just below the diagrams.

2. Plot of ground state energy (in unit of J) vs. inverse system size for ferric wheels up to Fe_{12}.

3. Plot of lowest energy (in unit of J) in every total spin sector vs. the total spin (S_{tot}) in case of Fe_{12}. It clearly obeys Taft's conjecture.

4. Plot of energy (in unit of J) vs. momentum vector k for Fe_6, Fe_8, Fe_{10} and Fe_{12}.

5. (a) Plot of static structure factor (S_q (in arbitary units)) for Fe_6 in all the subspaces. Here ground state lies in B^+ subspace. In (b), (c) and (d) we have plotted the static structure factor in A and B subspaces for Fe_8, Fe_{10} and Fe_{12} respectively. In the doubly degenerate subspaces the weight of S(q) is much smaller than that in the ground state.

6. Plot of evolution of magnetization in presence of an alternating axial magnetic field of three different amplitudes (H_0(in unit of $J/\hbar$)).

7. Field amplitude (H_0) dependence of frequency Ω (defined in the text). Dotted line shows the exponential nature of Ω_{max}.

8. Plot of $\hat{y}$ component of torque (in unit of $\frac{J}{\hbar - rad}$)with change in magnetic field applied at $\theta = \pi/4$.

(a)

$$\left(\tfrac{1}{2}\right) \quad \left(-\tfrac{1}{2}\right) \quad \left(\tfrac{1}{2}\right) \quad \left(-\tfrac{1}{2}\right) \quad \left(\tfrac{1}{2}\right) \quad \left(\tfrac{1}{2}\right)$$

$$1 \quad 0 \quad 1 \quad 0 \quad 1 \quad 1$$

$$\mathrm{I} = 43$$

(b)

$$\left(-\tfrac{3}{2}\right) \quad \left(\tfrac{5}{2}\right) \quad \left(\tfrac{3}{2}\right) \quad \left(\tfrac{1}{2}\right) \quad \left(\tfrac{5}{2}\right) \quad \left(\tfrac{1}{2}\right) \quad \left(-\tfrac{1}{2}\right) \quad \left(-\tfrac{3}{2}\right) \quad \left(-\tfrac{5}{2}\right) \quad \left(-\tfrac{1}{2}\right) \quad \left(-\tfrac{3}{2}\right) \quad \left(\tfrac{1}{2}\right)$$

$$001 \quad 101 \quad 100 \quad 011 \quad 101 \quad 011 \quad 010 \quad 001 \quad 000 \quad 010 \quad 001 \quad 011$$

$$\mathrm{I} = 14557188235$$

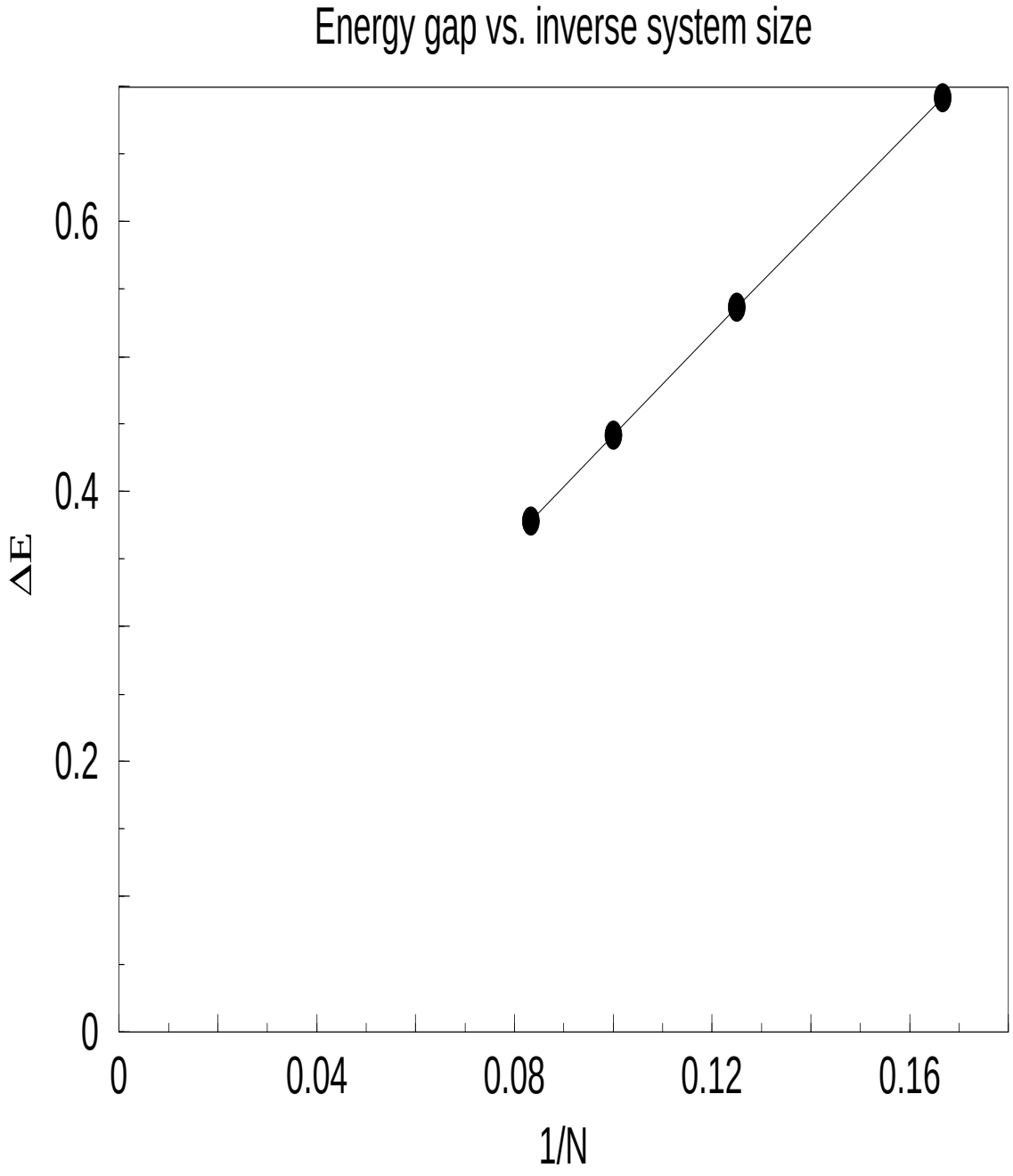

Energy gap vs. inverse system size
ΔE
0.6
0.4
0.2
0
0
0.04
0.08
0.12
0.16
1/N

Fig. 2

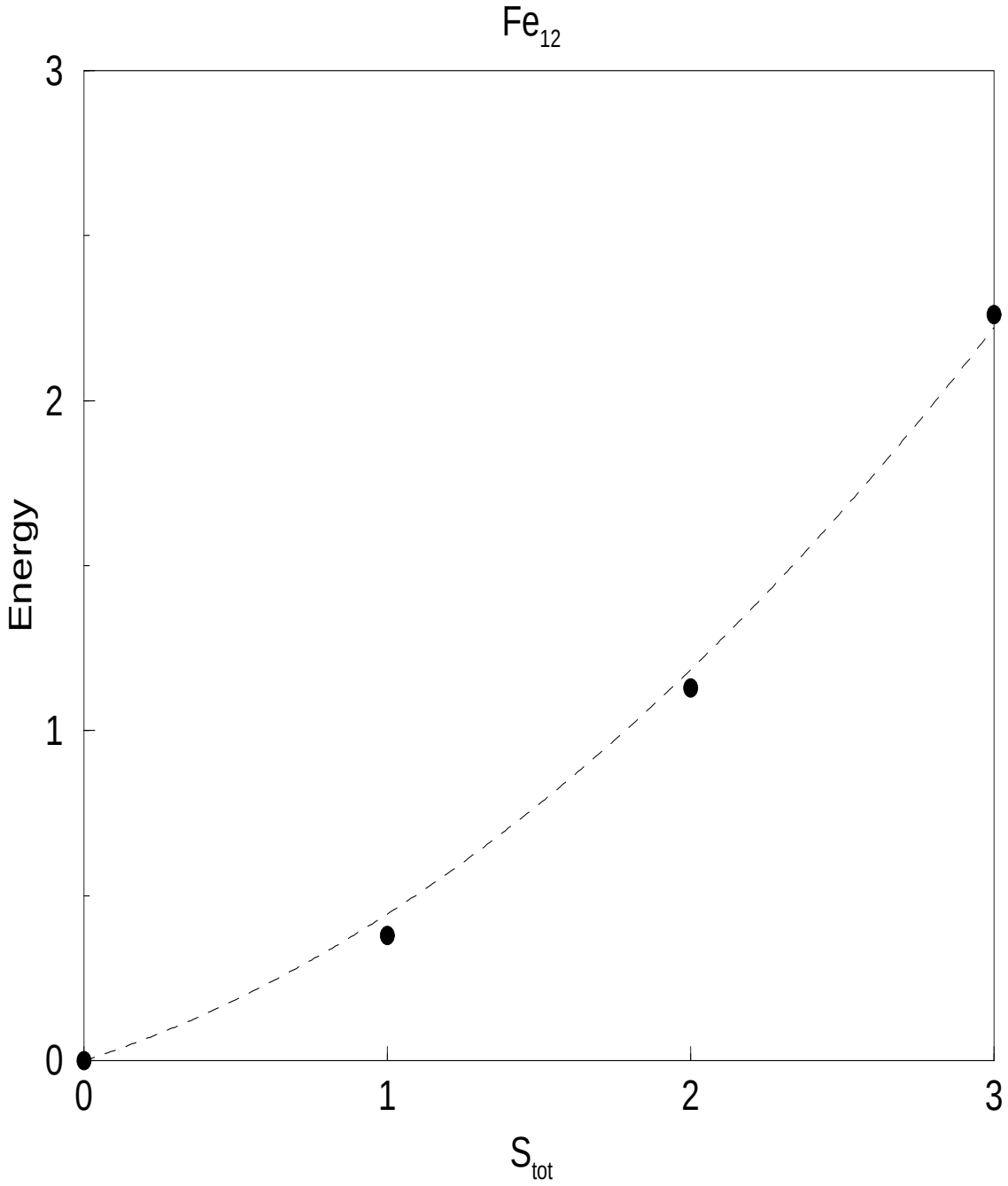


Fig. 3

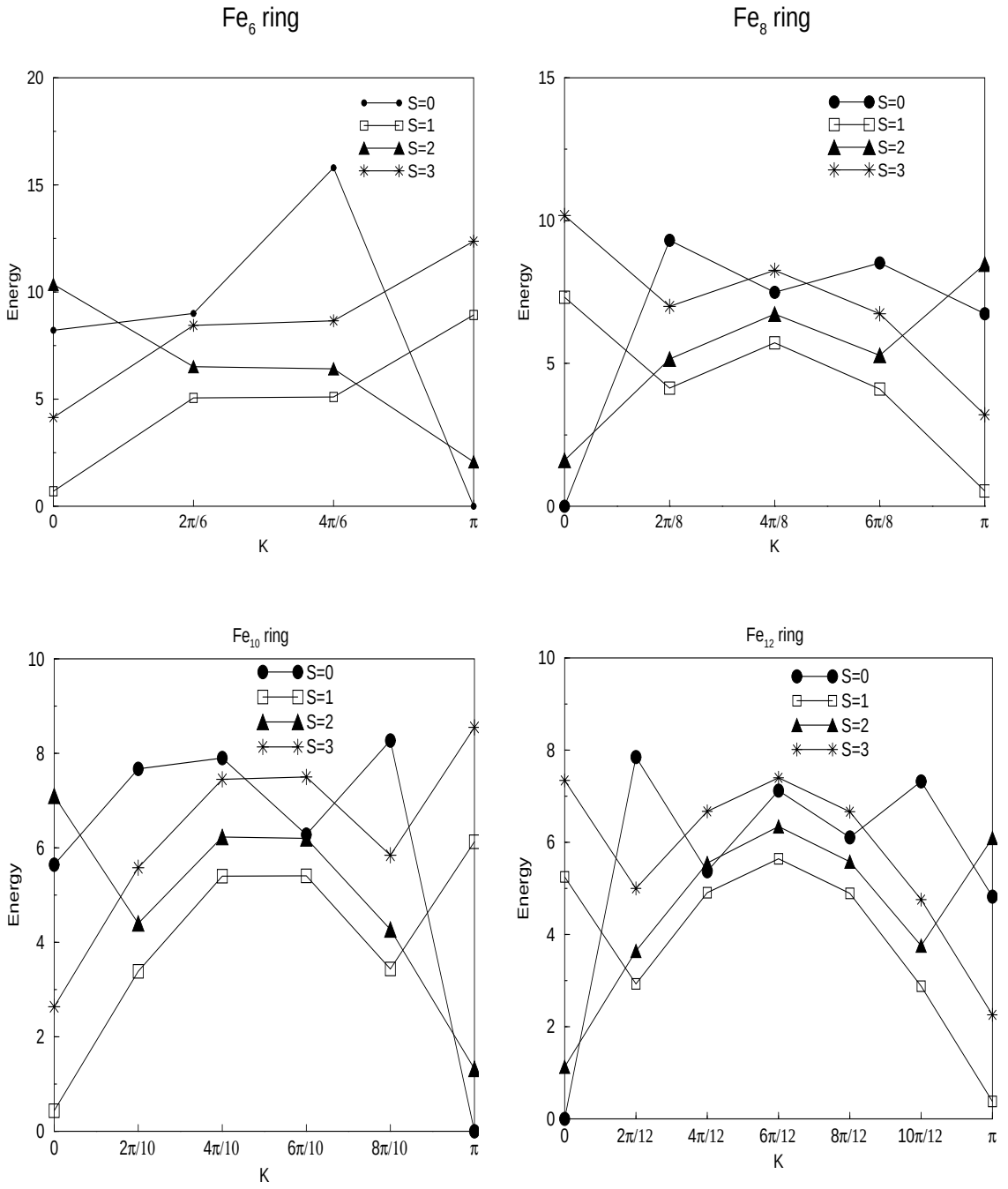

Fe6 ring
Fe8 ring
Fe10 ring
Fe12 ring
S=0
S=1
S=2
S=3
Energy
K
0
2π/6
4π/6
π
2π/8
4π/8
6π/8
2π/10
4π/10
6π/10
8π/10
2π/12
4π/12
6π/12
8π/12
10π/12

Fig. 4

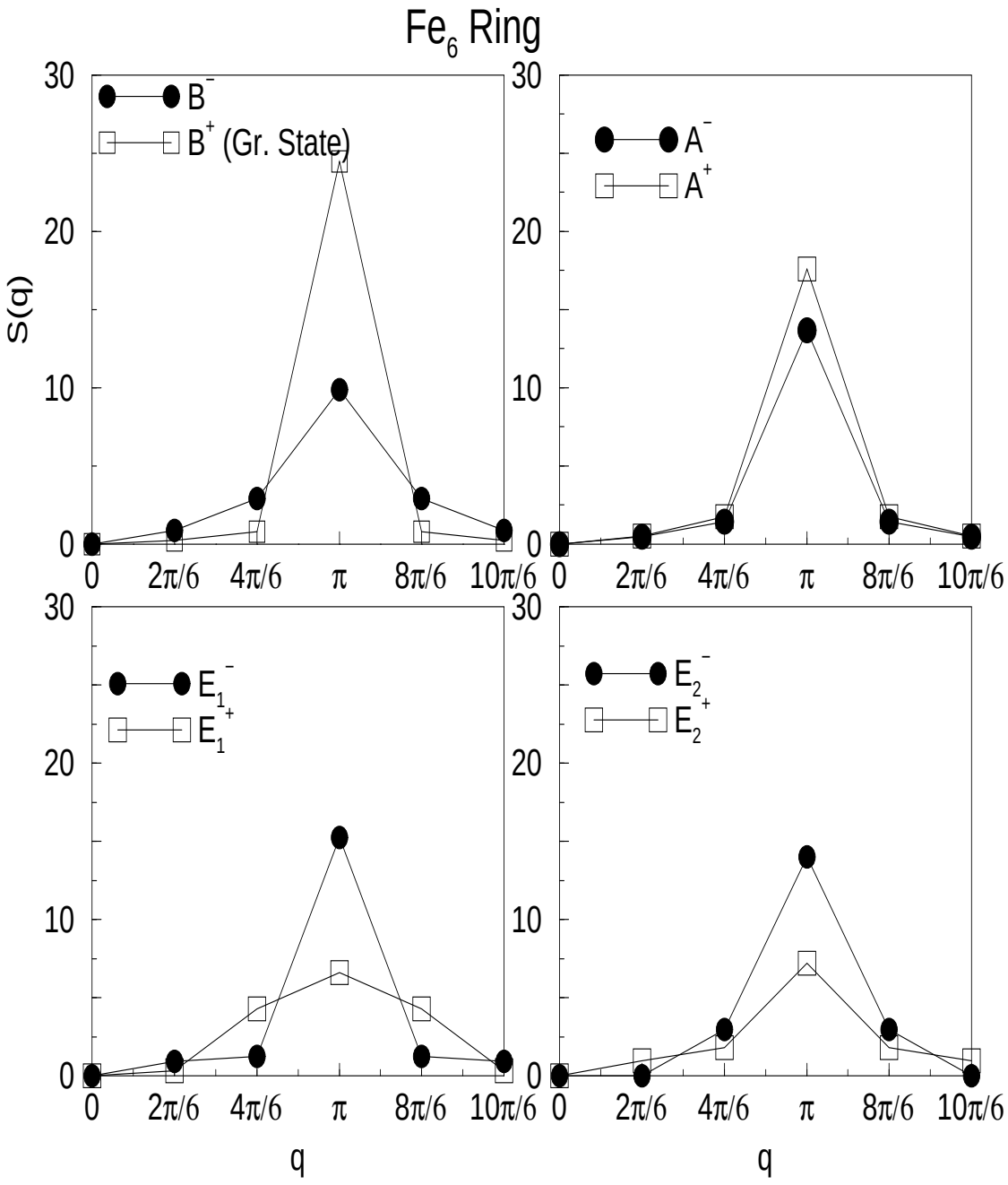

Fe6 Ring
S(q)
B−
B+ (Gr. State)
A−
A+
E1−
E1+
E2−
E2+
0
10
20
30
0
2π/6
4π/6
π
8π/6
10π/6
q

Fig. 5 (a)

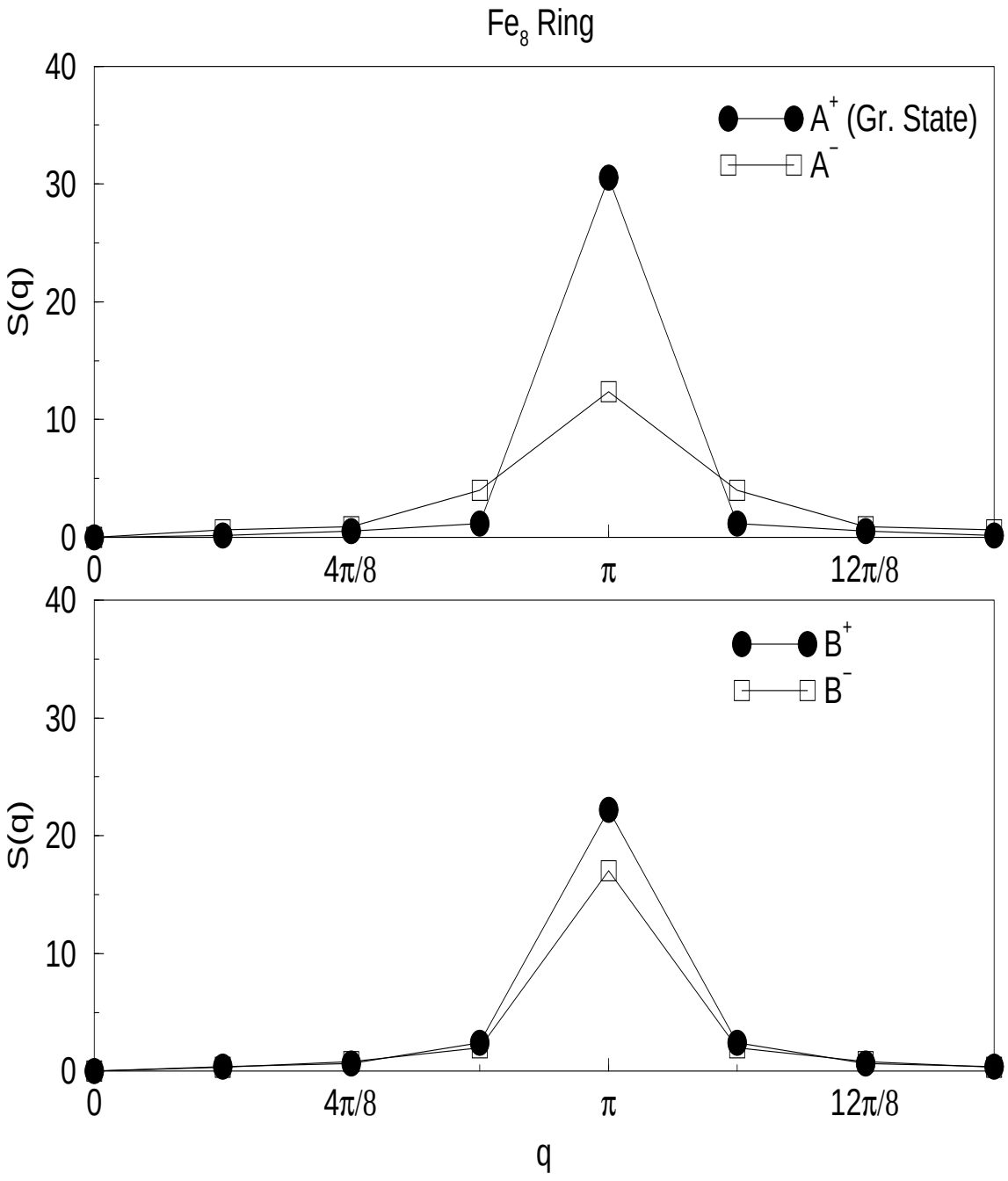


Fig. 5 (b)

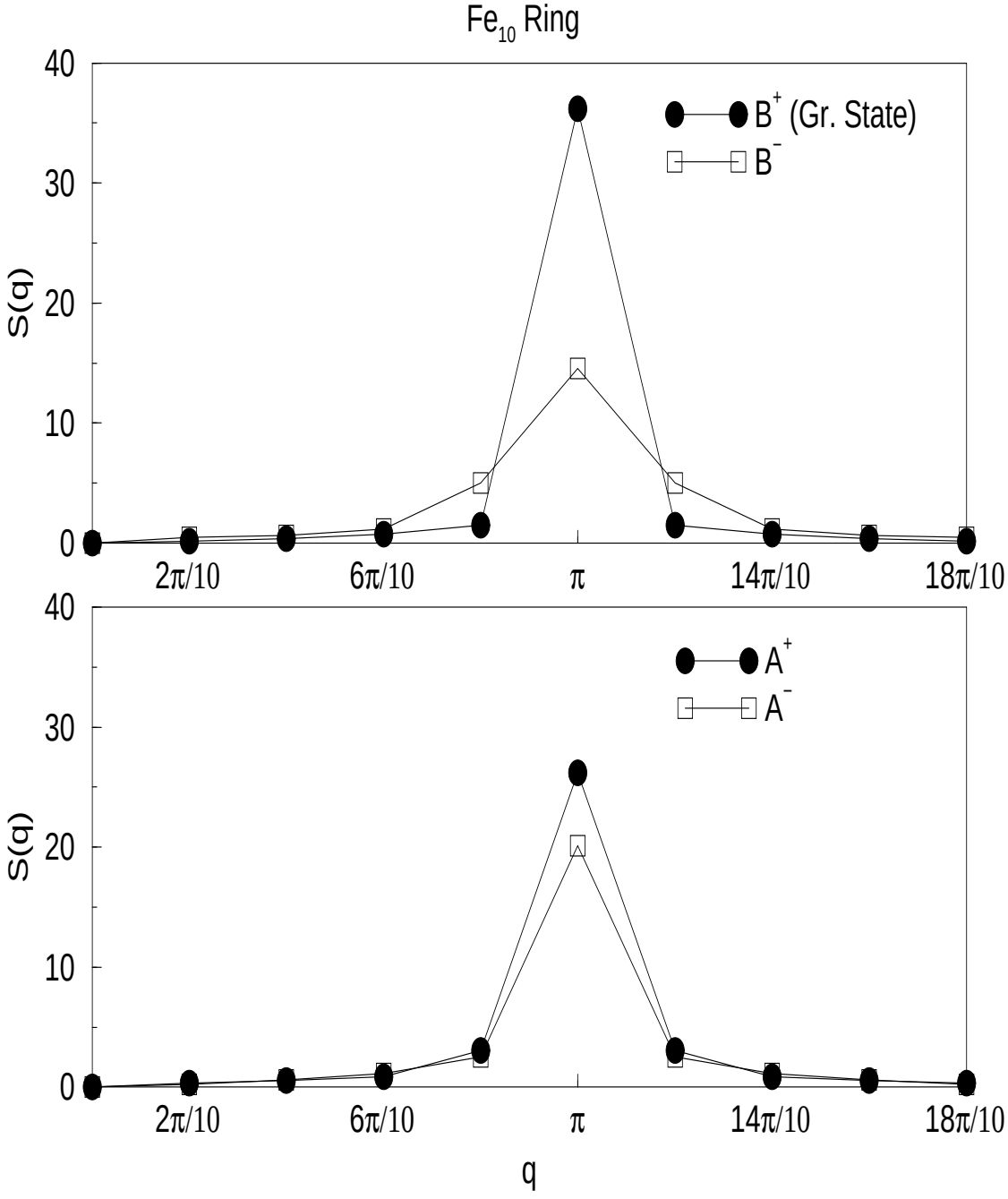

Fe10 Ring
B+ (Gr. State)
B-
A+
A-
S(q)
S(q)
0
10
20
30
40
2π/10
6π/10
π
14π/10
18π/10
q

Fig. 5 (c)

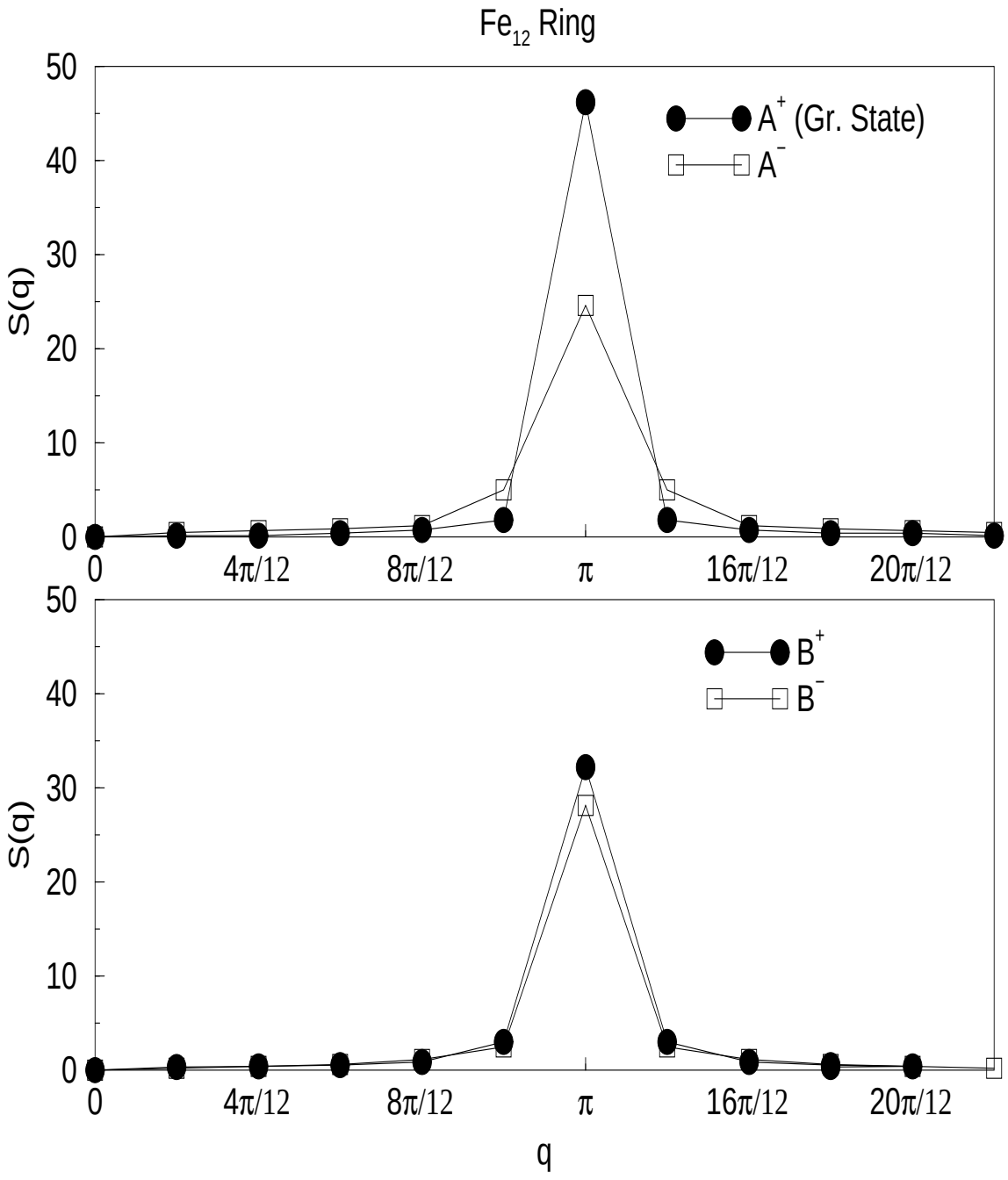

Fe12 Ring
A+ (Gr. State)
A−
B+
B−
S(q)
S(q)
q
0
4π/12
8π/12
π
16π/12
20π/12
50
40
30
20
10
0

Fig. 5 (d)

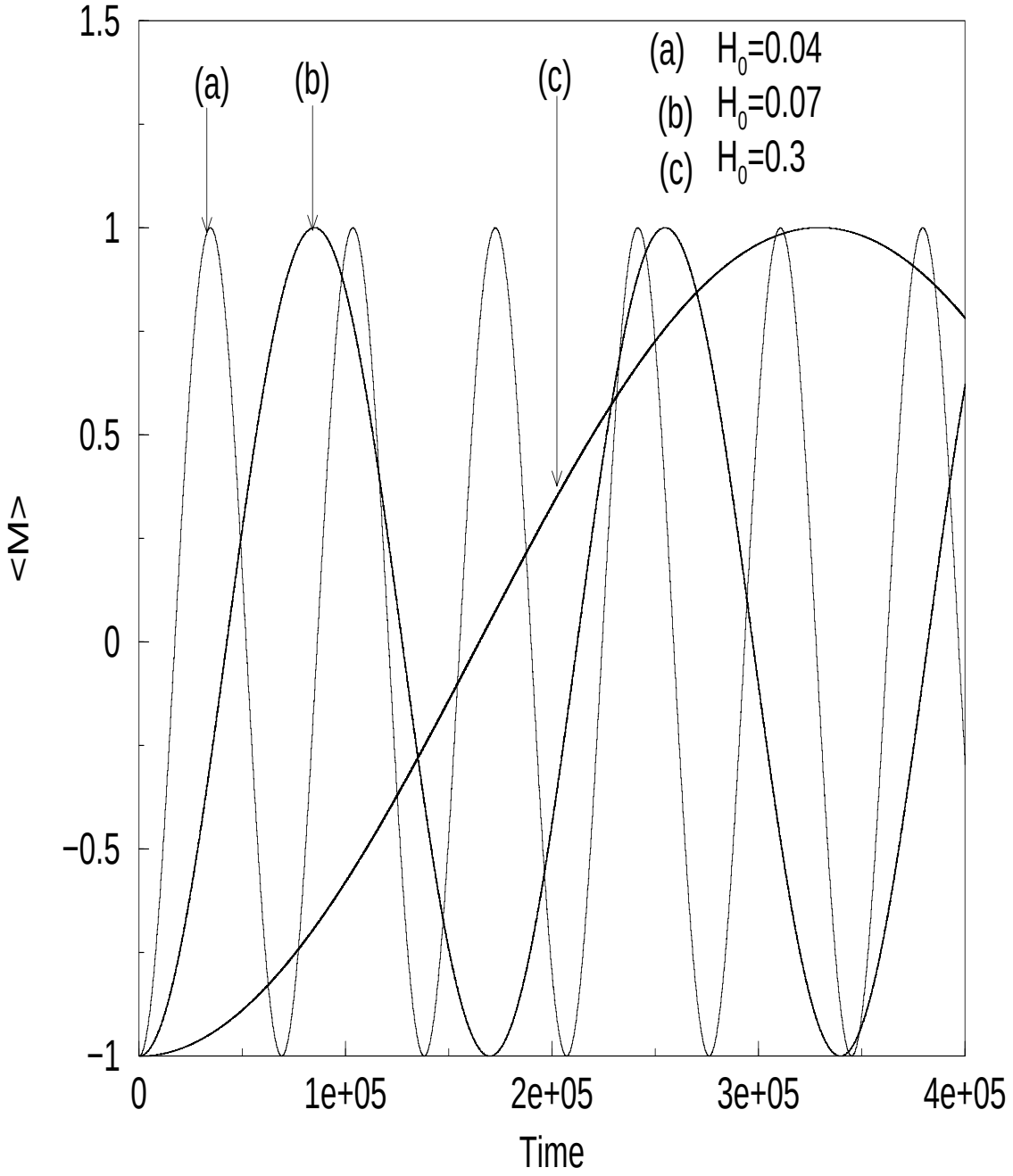

1.5
1
0.5
0
−0.5
−1
<M>
0
1e+05
2e+05
3e+05
4e+05
Time
(a)
(b)
(c)
(a) H0=0.04
(b) H0=0.07
(c) H0=0.3

Fig. 6

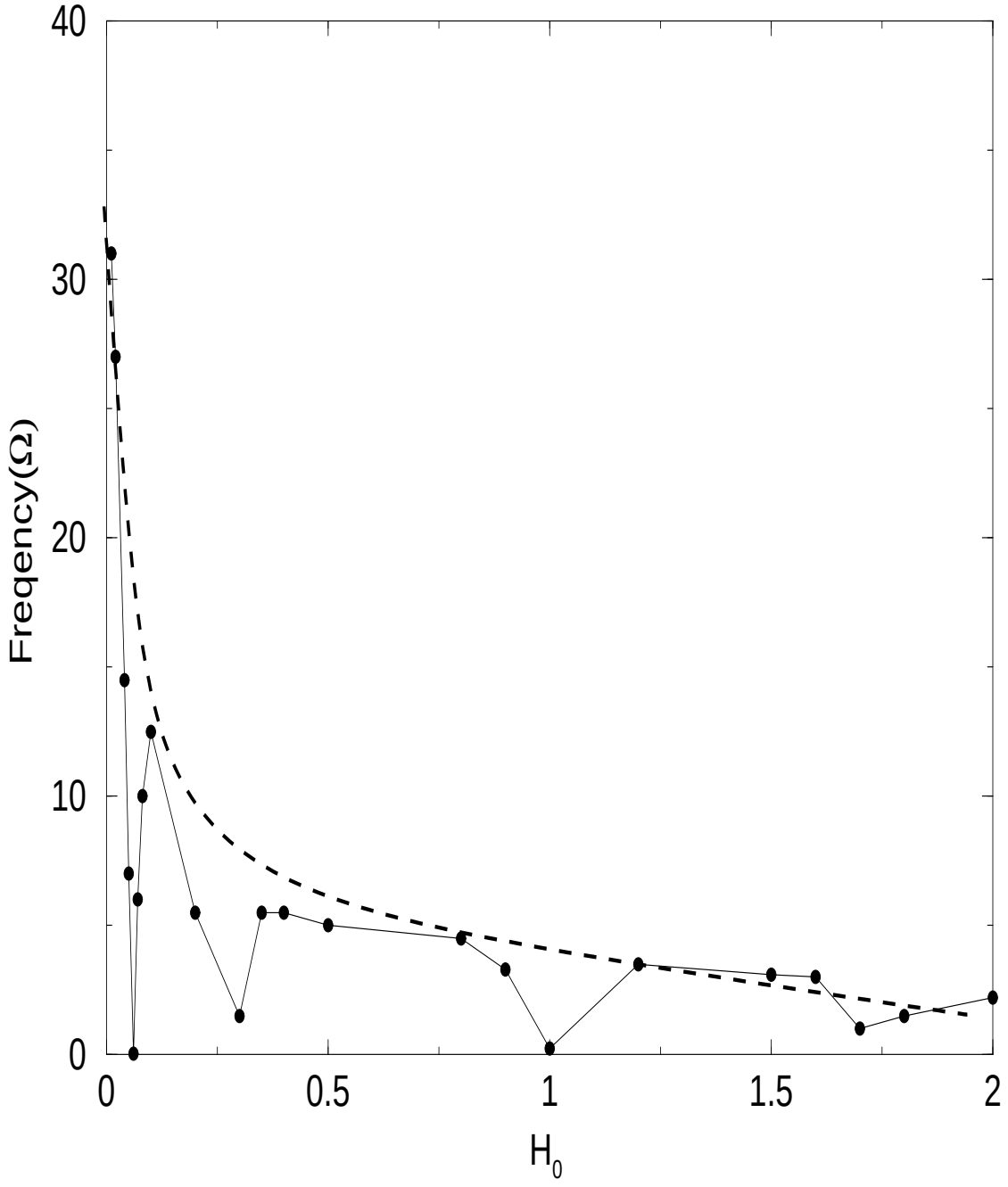


Fig. 7

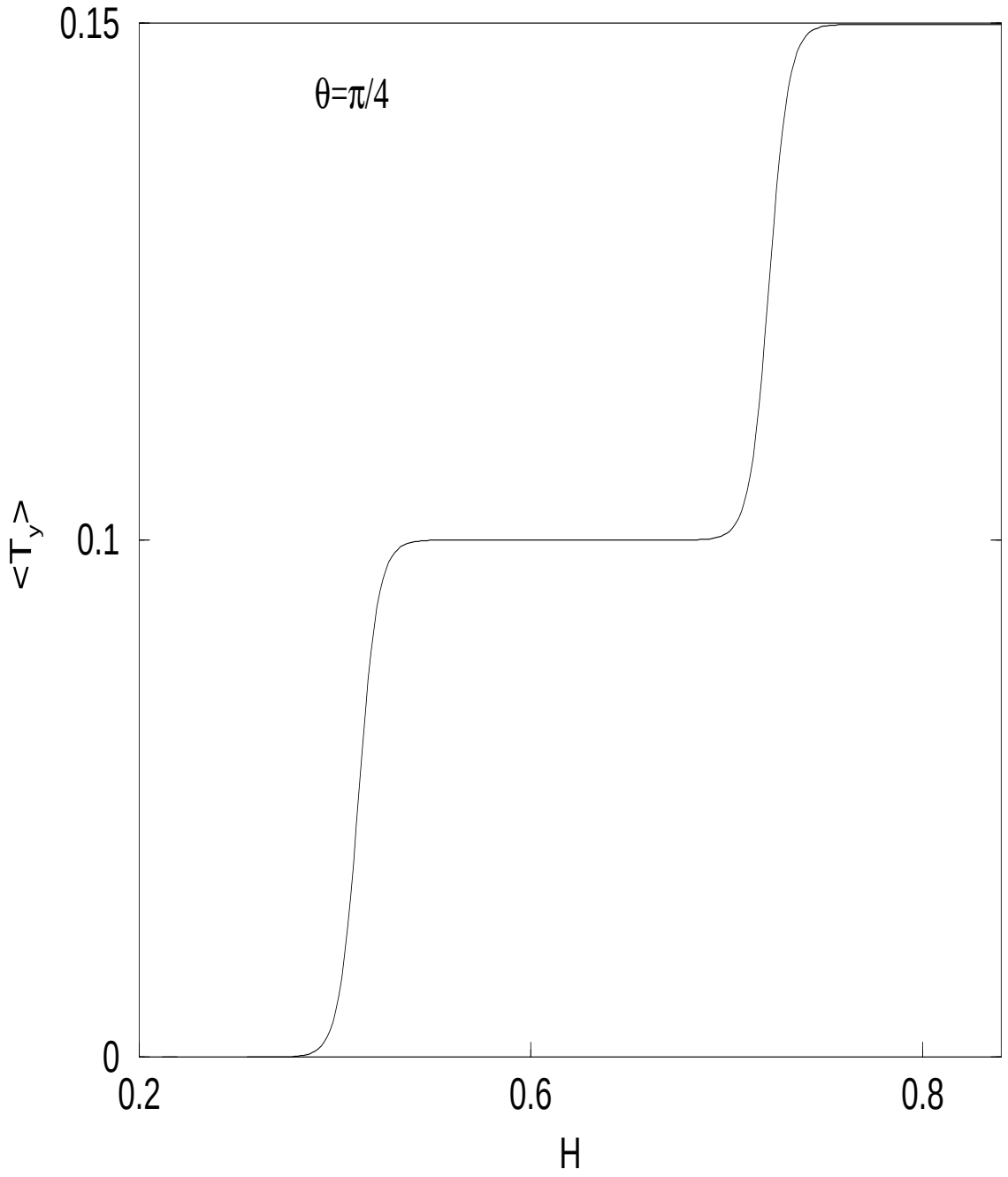


Fig. 8